

## Immune phenotypes and target antigens of clonally expanded bone marrow T cells in treatment-naïve multiple myeloma

Carlotta Welters<sup>1</sup>, María Fernanda Lammoglia Cobo<sup>1</sup>, Christian Alexander Stein<sup>1</sup>, Meng-Tung Hsu<sup>2</sup>, Amin Ben Hamza<sup>1</sup>, Livius Penter<sup>1,3</sup>, Xiaojing Chen<sup>2</sup>, Christopher Buccitelli<sup>4</sup>, Oliver Popp<sup>4</sup>, Philipp Mertins<sup>4</sup>, Kerstin Dietze<sup>1</sup>, Lars Bullinger<sup>1,5</sup>, Andreas Moosmann<sup>6,7</sup>, Eric Blanc<sup>8</sup>, Dieter Beule<sup>8</sup>, Armin Gerbitz<sup>9</sup>, Julian Strobel<sup>10</sup>, Holger Hackstein<sup>10</sup>, Hans-Peter Rahn<sup>11</sup>, Klaus Dornmair<sup>12</sup>, Thomas Blankenstein<sup>2</sup>, Leo Hansmann<sup>1,5</sup>

<sup>1</sup>Department of Hematology, Oncology, and Tumor Immunology, Charité – Universitätsmedizin Berlin, corporate member of Freie Universität Berlin and Humboldt-Universität zu Berlin, Berlin, Germany

<sup>2</sup>Molecular Immunology and Gene Therapy, Max-Delbrück-Center for Molecular Medicine (MDC) Berlin, Germany

<sup>3</sup>Dana-Farber Cancer Institute, Boston MA, USA

<sup>4</sup>Proteomics Platform, Max-Delbrück-Center for Molecular Medicine and Berlin Institute of Health, Robert-Rössle-Str. 10, 13125, Berlin, Germany

<sup>5</sup>German Cancer Consortium (DKTK), partner site Berlin, and German Cancer Research Center (DKFZ), Heidelberg, Germany

<sup>6</sup>Department of Medicine III, Klinikum der Universität München, Munich, Germany

<sup>7</sup>German Center for Infection Research (DZIF), Munich, Germany

<sup>8</sup>Core Unit Bioinformatics, Berlin Institute of Health, Berlin, Germany

<sup>9</sup>Hans Messner Allogeneic Stem Cell Transplant Program, Princess Margaret Cancer Centre, Toronto, Canada

<sup>10</sup>Department of Transfusion Medicine and Hemostaseology, Friedrich-Alexander-University Erlangen-Nuremberg, Erlangen, Germany

<sup>11</sup>Preparative Flow Cytometry, Max-Delbrück-Centrum für Molekulare Medizin, Berlin, Germany

<sup>12</sup>Institute of Clinical Neuroimmunology, University Hospital and Biomedical Center, LMU Munich, Germany

### Running title: T-cell phenotypes and targets in multiple myeloma

#### Correspondence:

Priv.-Doz. Dr. med. Leo Hansmann, MD

Charité – Universitätsmedizin Berlin (CVK)

Department of Hematology, Oncology, and Tumor Immunology

Augustenburger Platz 1

13353 Berlin, Germany

email: leo.hansmann@charite.de

phone: +49-(0)30-450-665238

fax: +49-(0)30-450-553914

#### Conflict of interest disclosure statement:

Lars Bullinger: Advisory Committees: Abbvie, Amgen, Astellas, Bristol-Myers Squibb, Celgene, Daiichi Sankyo, Gilead, Hexal, Janssen, Jazz Pharmaceuticals, Menarini, Novartis, Pfizer, Sanofi, Seattle Genetics; Research support Bayer and Jazz Pharmaceuticals.

All other authors declare no competing financial interests.

## SYNOPSIS

Bone marrow T-cell clonal expansion, immune phenotypes, and specificities at the single-cell level were determined in treatment-naïve multiple myeloma. Dominant T-cell clones rarely recognize antigens presented on myeloma cells, are not neoantigen-specific, and show low immune checkpoint expression.

## ABSTRACT

Multiple myeloma is a hematologic malignancy of monoclonal plasma cells that accumulate in the bone marrow. Despite their clinical and pathophysiological relevance, the roles of bone marrow-infiltrating T cells in treatment-naïve patients are incompletely understood. We investigated whether clonally expanded T cells i) were detectable in multiple myeloma bone marrow, ii) showed characteristic immune phenotypes, and iii) whether dominant clones recognized antigens selectively presented on multiple myeloma cells. Single-cell index sorting and T-cell receptor (TCR)  $\alpha\beta$  sequencing of bone marrow T cells from 13 treatment-naïve patients showed dominant clonal expansion within CD8 $^{+}$  cytolytic effector compartments, and only a minority of expanded T-cell clones expressed the classical immune checkpoint molecules PD-1, CTLA-4, or TIM-3. To identify their molecular targets, TCRs of 68 dominant bone marrow clones from five selected patients were re-expressed and incubated with multiple myeloma and non-multiple myeloma cells from corresponding patients. Only one out of 68 TCRs recognized antigen presented on multiple myeloma cells. This TCR was HLA-C-restricted, self-peptide-specific, and could be activated by multiple myeloma cells of multiple patients. The remaining dominant T-cell clones did not recognize multiple myeloma cells and were, in part, specific for antigens associated with chronic viral infections. In conclusion, we showed that dominant bone marrow T-cell clones in treatment-naïve patients rarely recognize

antigens presented on multiple myeloma cells and exhibit low expression of classical immune checkpoint molecules. Our data provide experimental context for experiences from clinical immune checkpoint inhibition trials and will inform future T cell-dependent therapeutic strategies.

## INTRODUCTION

Multiple myeloma is a hematologic malignancy characterized by accumulation of monoclonal plasma cells in the bone marrow. Immune cells constituting the bone marrow microenvironment have a major role in disease pathophysiology (1-3), and immunomodulatory agents, as well as monoclonal antibodies, are part of effective treatment regimens (4,5).

Clonal T-cell expansion is an antigen-driven process, and the roles of clonally expanded multiple myeloma-infiltrating T cells are incompletely understood. In solid tumors, neoantigens can drive specific clonal T-cell expansion, resulting in functionally exhausted T-cell compartments (6-9). The peripheral blood of heavily pre-treated multiple myeloma patients can contain variable amounts of neoantigen-specific T cells (10); however, their occurrence in the bone marrow of treatment-naïve patients, degrees of clonal expansion, impact on multiple myeloma pathophysiology, and clinical significance remain unclear. Tumor mutational burden, which correlates with presence of tumor-specific T cells and response to immune checkpoint inhibition in solid tumors, can be considered intermediate in multiple myeloma (11) and increases with the number of previous treatment regimens. T cells can recognize multiple myeloma-associated antigens but acquire features of functional inhibition during disease progression (12,13). However, immune checkpoint blockade targeting PD-1/PD-L1 interactions to reverse functional T-cell inhibition has been ineffective as a monotherapy in multiple myeloma (14) and has led to increased severe adverse events without improving clinical responses in combination therapies (15,16). Furthermore, multiple myeloma cells can reduce antigen presentation (17), and regulatory T cells (Tregs) may contribute to the impairment of effective anti-myeloma T cell responses (18).

Hypothesizing that T-cell expansion can be driven by chronically persisting multiple myeloma-associated antigens, we studied differentiation states and specificities of dominant bone marrow T-cell clones in treatment-naïve patients at the single-cell level. We investigated whether i) clonal expansion was restricted to bone marrow T cells, ii) clonal T-cell expansion associated with characteristic immune phenotypes, and iii) dominant bone marrow T-cell clones recognized antigens selectively presented on multiple myeloma cells.

## MATERIALS AND METHODS

### Patient and healthy donor samples

The study was approved by the local institutional review board (Ethikkommission der Charité, protocol EA2/096/15 to LH). All patients and one healthy peripheral blood donor were accrued at Charité – Universitätsmedizin Berlin, provided written informed consent, and all research was conducted in accordance with the Declaration of Helsinki. All samples were acquired between August 2015 and October 2019. None of the participants had clinically apparent signs of infection at the time of sample collection. Bone marrow mononuclear cells and peripheral blood mononuclear cells (PBMCs), if available, were isolated using Ficoll-Paque PLUS (GE Healthcare) according to the manufacturer's instructions and were cryopreserved in RPMI 1640 (ThermoFisher Scientific) containing 50% fetal bovine serum (FBS, ThermoFisher Scientific) and 10% dimethyl sulfoxide (DMSO, Carl Roth GmbH) before further processing. For cryopreservation, vials were stored in liquid nitrogen. Patient characteristics and genetic features are listed in Table 1 and Supplementary Table S1, respectively.

### Fluorescence-activated cell sorting (FACS)

Cells isolated from bone marrow, peripheral blood, and cell lines were stained with multi-parameter panels according to the manufacturer's instructions. Briefly, up to  $5 \times 10^6$  cells were washed in pure phosphate-buffered saline (PBS, ThermoFisher Scientific), centrifuged at 300 x g, supernatant was decanted, and cells were stained with the indicated antibodies at 4 °C for 30 minutes protected from light. After staining, cells were washed with PBS containing 2% (FBS, ThermoFisher Scientific) and re-suspended in 100 µL PBS containing 2% FBS for subsequent analysis or sorting. Index sorting for single-cell sequencing was done using a FACS Aria Fusion high-speed cell sorter (BD Biosciences) equipped with a 70 µm nozzle as previously described (19,20). Antibodies used for index sorting are listed in Supplementary Table S2. Flow cytometry for cell analysis was performed using LSR Fortessa (BD Biosciences), Navios (Beckman Coulter), or Aurora (Cytek) instruments.

### T-cell receptor (TCR)αβ, cytokine, and transcription factor sequencing

Single-cell nucleic acid amplification, library preparation, sequencing, and data processing were done as described previously (19-22). For peripheral blood bulk TCRβ repertoire sequencing, we used the T-cell receptor beta (TCRB) Deep immunoSEQ assay (Adaptive biotechnologies) with 10 µg PBMC DNA per patient as input.

### Single-cell gene expression to determine cell type-associated *AP5M1* expression

Single-cell gene expression, VDJ immunoglobulin sequencing, and feature barcoding of bone marrow mononuclear cells and PBMCs to illustrate cell type-associated *AP5M1* expression were done using the Chromium Single Cell Immune Profiling platform, Chromium Next GEM Single Cell 5' Kit v2, Chromium Single Cell Human BCR Amplification Kit, and 5' Feature Barcode Kit (all 10x Genomics) according to the manufacturer's instructions. For feature barcoding, cells were stained with the following antibodies according to the manufacturer's instructions: CD38 (RRID: AB\_2800758), CD138 (RRID: AB\_2810567), CD45 (RRID: AB\_2800762), CD56 (RRID: AB\_2801024), CD19 (RRID: AB\_2800741), CD20 (RRID: AB\_2800743), CD3 (RRID: AB\_2800723), CD14 (RRID: AB\_2810576), TIM-3 (RRID: AB\_2800925), BTLA (RRID: AB\_2800919), PD-1 (RRID: AB\_2800862), CD39 (RRID: AB\_2800853), CD8 (RRID: AB\_2800922), CXCR4 (RRID: AB\_2800791), CD57 (RRID: AB\_2801030) (all BioLegend). Sequencing was done on a NovaSeq 6000 system (Illumina) with the following specifications: Single cell gene expression was sequenced 27 x 97 bp paired end, feature barcodes and BCR sequences were sequenced 27 x 92 bp paired end. Numbers of sequenced cells are indicated in the respective figure descriptions. Cellranger 5.0.1, Loupe Browser 5.0, and Loupe VDJ Browser 4.0 (all 10x Genomics) were used for data processing and illustration according to the manufacturer's instructions.

### **Identification of somatic mutations**

DNA and RNA were isolated from study patients' multiple myeloma bone marrow cells using the AllPrep DNA/RNA micro kit or QIAamp DNA mini kit (both Qiagen). PBMC DNA of the respective patients was used as germline control. In cases where peripheral blood was not available as a germline control (patients MM003 and MM165), bone marrow was

CD38-depleted by MACS, as described below, and subsequently CD38<sup>-</sup>CD138<sup>-</sup>CD19<sup>-</sup> cells were sorted via FACS as specified.

For DNA library preparations, we used SureSelect Human All Exome V7 kits (Agilent), for RNA library preparation, TruSeq Stranded mRNA kits (Illumina) were used. DNA was sequenced 100 bp paired end or 150 bp paired end, RNA was sequenced 75 bp paired end, all on a HiSeq 4000 (Illumina). Sequencing data were mapped against the human genome release GRCh37 with decoy regions (hs37d5). BWA (23) was used to align exome data, STAR (24) to align mRNA data, applying the GENECODE release 19 as annotations. Somatic single nucleotide variants (SNVs) were detected using MuTect (25). The median sequencing depth of exome data was 215x for 13 samples sequenced with 100 cycles, and 629x for 5 samples sequenced with 150 cycles. The median number of reads for expression data was  $3.33 \times 10^8$  reads/sample. Presentation of expressed mutations was predicted using NetMHC 4.0 and NetMHCpan 4.0 (26). Peptides with affinity < 1000 nM and/or %Rank  $\leq 2$  were considered presented.

### Magnetic-activated cell separation (MACS)

Multiple myeloma cells from patient bone marrow were magnetically enriched using the Plasma Cell Isolation Kit II, human (Miltenyi Biotec) according to the manufacturer's instructions with the following modification: only CD38 MicroBeads from the Plasma Cell Isolation Kit II, human (Miltenyi Biotec) were used and positive selection was applied. For enrichment of CD8<sup>+</sup> TCR-transduced T cells, we performed depletion of CD4<sup>+</sup> T cells immediately before co-incubation experiments, using the CD4 MicroBeads, human kit (Miltenyi Biotec).

## Cell lines

Multiple myeloma cell lines U266B1 (RRID: CVCL\_0566), JJN-3 (RRID: CVCL\_2078), L-363 (RRID: CVCL\_1357), NCI-H929 (RRID: CVCL\_1600), and KMS-12-PE (RRID: CVCL\_1333), as well as HEK293T (RRID: CVCL\_0063), were provided by the Blankenstein laboratory.  $58\alpha^- \beta^-$  T hybridoma cells were created by the Dornmair laboratory (27) and kindly provided in 2019. For all experiments, cryopreserved vials of the respective cell lines were thawed and cultivated at 37 °C and 5% CO<sub>2</sub> for 7-14 days before further use. All cell lines were authenticated by microscopy and flow cytometry, and absence of mycoplasma was confirmed by LookOut Mycoplasma PCR-Detections-Kit (Sigma-Aldrich). All cell lines were cultured in RPMI1640 containing 10% FBS, 10000 U/mL penicillin, 10 mg/mL streptomycin (all ThermoFisher Scientific).

## TCR expression on human peripheral blood lymphocytes

TCR gene transfer for recombinant TCR expression was performed as previously described (28) with minor modifications: All TCR $\alpha\beta$  chains (Supplementary Table S3) were linked via a self-cleaving peptide (P2A, amino acid sequence: ATNFSLLKQAGDVEENPGP), and human TCR constant regions were replaced by their murine counterparts as described previously (29). All TCR DNA sequences (Supplementary Table S3) were codon-optimized for mammalian expression and synthesized (GeneArt, Life Technologies).

## TCR expression on $58\alpha^- \beta^-$ reporter cells

All TCR DNA sequences (Supplementary Table S3) were synthesized (GeneArt, Life Technologies). TCRs were expressed on  $58\alpha^- \beta^-$  T hybridoma cells, which also expressed human

CD8 $\alpha\beta$  chains and green fluorescent protein (GFP) under the control of nuclear factor of activated T cells (NFAT), as described (21,27). These cells are referred to as “58 $\alpha^- \beta^-$ ” reporter cells. Recombinant TCR expression was confirmed by CD3 staining (Brilliant Violet 421 anti-mouse CD3, BioLegend, RRID: AB\_10900227) according to the manufacturer’s instructions.

### T-cell stimulation, incubation with potential target cells, and target peptide identification

60000 TCR-recombinant 58 $\alpha^- \beta^-$  cells were stimulated with plate-bound anti-mouse CD3 (clone 17A2, BioLegend, RRID: AB\_2810314) for 16 h at 37 °C and 5% CO<sub>2</sub> as a positive control. Mouse IL2 secretion was measured using the Mouse IL2 Duo Set ELISA Kit (R&D Systems) according to the manufacturer’s instructions. Activation of TCR-transduced human PBL was detected using the Human IFN $\gamma$  ELISA Set BD OptEIA (BD Biosciences, RRID: AB\_2869029) according to the manufacturer’s instructions. ELISA plates were analyzed using the Infinite M Plex (Tecan) plate reader, and Magellan (Tecan) data analysis software version 7.0. Co-incubation details are listed in Supplementary Table S4.

Potential target peptides (predicted from the somatic mutation data as indicated) were synthesized (JPT Peptide Technologies GmbH or GenScript Biotech Corporation) and loaded onto L-363 as antigen-presenting cells at 5  $\mu$ M concentration. For each co-incubation with TCR-recombinant T cells, 100000 L-363 were used. For target peptide screening and co-incubation with multiple myeloma cells, TCRs specific for cytomegalovirus-derived peptides (TPR, amino acid sequence: TPRVTGGGAM; or VTE, amino acid sequence: VTEHDTLLY), and an Epstein-Barr virus-derived peptide (GLC, amino acid sequence: GLCTLVAML) were used as positive controls. The sequences of the TPR-specific TCR are derived from MM008 15E10, and the VTE-specific TCR from MM139 10F7 (Supplementary Table S3); the GLC-specific TCR was

previously published (30). CDR3 amino acid sequences of all TCRs detailed in Supplementary Table S3 were screened for potential target epitopes using VDJdb (<https://vdjdb.cdr3.net>).

All co-incubations of TCR-recombinant and bone marrow cells (Supplementary Table S4) were performed in 96-well plates in 150 µL RPMI1640 containing 10% FBS, 10 000 U/ml penicillin, and 10 mg/ml streptomycin (all ThermoFisher Scientific) for 16 hours at 37 °C and 5% CO<sub>2</sub>. For target peptide screening, we generated pools of eight Micro-Scale Peptides (JPT Peptide Technologies GmbH) and added a cytomegalovirus pp65-derived control peptide (TPRVTGGGAM, called TPR, presented on HLA-B\*07:02, GenScript Biotech Corporation). All peptide pools (final concentration of 1-5 µM per peptide) were incubated with 60000 reporter cells expressing the TCR in question or a control peptide-specific TCR for 16 hours at 37 °C and 5% CO<sub>2</sub>. In case of T-cell activation determined by GFP fluorescence, each peptide in the respective pool was tested individually and activating peptides were synthesized with high purity (GenScript Biotech Corporation) for verification. For HLA-blocking, purified antibodies against HLA-A2 (clone BB7.2, BioLegend, RRID: AB\_1659243), HLA-BC (clone B1.23.2, ThermoFisher Scientific, RRID: AB\_2866114), or HLA-class I (clone W6/32, BioLegend, RRID: AB\_2561492) were titrated and used at the indicated concentrations. Ultra-LEAF Purified Mouse IgG2a κ isotype control (clone MOPC-173, BioLegend, RRID: AB\_11148947) or Purified Mouse IgG1 κ isotype control (clone MOPC-21, BioLegend, RRID: AB\_2891079) were used as isotype controls at the indicated concentrations.

### HLA knockout using CRISPR-Cas9

The following guide RNAs (5' → 3') were used for HLA knock-out: ACAGCGACGCCGAGCCAG (HLA-A), CGTACTGGTCATGCCCGCG (HLA-B), and

GACACAGAAGTACAAGCGCC (HLA-C). All guide RNAs were coded within pSpCas9 plasmids (GenScript). JJN-3 and U266B1 cells were transfected by electroporation (Gene Pulser Xcell, BioRad), and HEK293T were transfected with FuGENE® HD Transfection Reagent (Promega). HLA-knockout cell lines were expanded for 4-6 weeks from single cells sorted on a FACSaria Fusion high-speed cell sorter (BD Biosciences) equipped with a 70 µm nozzle. Cell culture conditions are specified in the cell lines section. HLA knockout was confirmed by flow cytometry using antibodies against HLA-B7 (clone BB7.1, BioLegend, RRID: AB\_2650776), HLA-C (clone DT9, BD Biosciences, RRID: AB\_2739715) or HLA-class I (clone W6/32, BioLegend, RRID: AB\_493669) according to the manufacturer's instructions.

### Recombinant HLA expression

HLA coding sequences (IPD accession numbers HLA00401, HLA00404, HLA00413, HLA00420, HLA01451, HLA00427, HLA00433, HLA00434, HLA01672, HLA00446, HLA00455, HLA00467) were downloaded from IPD-IMGT/HLA (<https://www.ebi.ac.uk/ipd/imgt/hla/blast.html>), synthesized (ThermoFisher Scientific), cloned into pHSE3' as previously described (27), and nucleofected (SF Cell Line 4D-Nucleofector® X Kit L, Lonza) into 250000 JJN-3 cells. HLA expression was confirmed by flow cytometry as detailed above.

### U266B1 gene expression and peptidome data

Multiple myeloma U266B1 gene expression data are publicly available (LL-100) (31) and were used. Published U266B1 peptidome data were provided by the authors (32) and combined with a dataset we generated as previously described (33) with minor modifications. Briefly,

1x10<sup>8</sup> U266B1 cells were lysed in 200 µL lysis buffer containing 1% cholamidopropyl dimethylammonio propanesulfate (CHAPS), 200 mM Tris-HCl, 150 mM NaCl, and 1x Halt Protease Inhibitor Cocktail (all ThermoFisher Scientific) for 60 minutes at 4 °C. The lysate was centrifuged at 13000 x g for 10 minutes, and the supernatant was incubated with HLA-class I-specific antibody (clone W6/32, BioLegend, RRID: AB\_2561492) at 60 µg/mL for 60 minutes at 4 °C. Recombinant (r)Protein A Sepharose Fast Flow beads (Sigma) were added at 100 µL beads/mL lysate and incubated for another 5 hours. Peptides were then eluted with 50 µL 10% acetic acid (Sigma) and desalted on C18 STAGE tips (ThermoFisher Scientific) as described previously (34). Peptides were taken up in 0.1% formic acid, 3% acetonitrile (both ThermoFisher Scientific), and acquired on an EASY-nLC 1200 system (Thermo Fisher Scientific) coupled to a Q Exactive HF-X orbitrap mass spectrometer (Thermo Fisher Scientific). Samples were separated on a 110-minute gradient ramping from 5 to 55% acetonitrile using an in-house prepared nano-LC column (0.074 mm x 250 mm, 1.9 µm Reprosil C18, Dr. A. Maisch HPLC GmbH) and a flow rate of 250 nL/minute. MS acquisition was operated in positive mode at an MS1 resolution of 60000 and a scan range from 350 to 1800 m/z. For data-dependent MS2 acquisition, the top 20 peaks were selected for MS2 with a resolution of 45000, a maximum injection time of 250 ms and an isolation window of 1.3 m/z. Automatic gain control (AGC) target was set to 1x10<sup>5</sup> and dynamic exclusion was specified to 30 sec. Raw files were analyzed in MaxQuant (version 1.6.2.6) (35) applying an unspecific search against a human Uniprot database (2017), which allowed a peptide length of 7-14 amino acids.

## Data availability statement

Detailed TCR sequence and mutation data can be found in the supplementary data. Whole exome and RNA-sequencing raw data are publicly available at sequence read archive (<https://www.ncbi.nlm.nih.gov/sra> under BioProject accession number PRJNA862671).

### Statistical analysis

Statistics were calculated using R (36) version 4.0.3. Applied tests and P value thresholds are indicated in all figure descriptions.

## RESULTS

### Multiple myeloma bone marrow is infiltrated with clonally expanded CD8<sup>+</sup> cytolytic effector T cells

We hypothesized that multiple myeloma could drive specific clonal T-cell expansion, and we determined 13-dimensional immune phenotypes and TCRαβ sequences of single bone marrow T cells from 13 treatment-naïve patients (Table 1, Suppl. Table S1). A total of 6744 bone marrow T cells (368-1288 T cells per patient) were FACS index sorted (gating in Suppl. Fig. S1, antibody panel in Suppl. Table S2). TCR sequences were determined in 5695 cells (84% of sorted cells), and clones were considered expanded if identical TCRαβ complementarity determining region 3 (CDR3) amino acid sequences were detected in at least two cells within a patient. Clones were defined as positive for a fluorescent parameter if the majority of cells were positive. The number of expanded T-cell clones varied across patients (range: 6-71 expanded clones per patient), with detailed data of two patients are shown as representative examples for relatively strong and weak clonal expansion in Figure 1A, and the number of expanded T-cell

clones within all patients was determined (Figure 1B). Clonal expansion predominantly occurred within CD8<sup>+</sup> compartments (Fig. 1C), and size of most expanded clones per patient ranged from 2–25% of CD8<sup>+</sup> T cells (Fig. 1D). Compared to non-expanded T cells, expanded clones were more frequently positive for CD57, while being less frequently positive for CCR7 and CD28 (Fig. 1E). Significant differentially expressed markers between expanded and non-expanded T cell clones are shown for patient MM160 as an example in Figure 1F (all patients in Suppl. Fig. S2). Regarding transcription factor and cytokine expression, *TBX21* and *GZMB* were more frequently expressed in clonally expanded compared to non-expanded T cells (Fig. 1G, all parameters in Suppl. Fig. S3). Expression of the immune checkpoint molecules PD-1, CTLA-4, and TIM-3 varied across patients but was not significantly different between expanded and non-expanded T-cell clones and was generally low on CD8<sup>+</sup> T-cell clones (Fig. 1E). In contrast, BTLA was expressed on more than 50% of T cells, irrespective of clonal expansion (Fig. 1E). Data on clone-associated immune phenotypes were consistent across technical replicates and not affected by total numbers of sequenced cells per patient (Suppl. Fig. S4). Taken together, immune phenotypes of expanded bone marrow T-cell clones were significantly different from those of non-expanded clones and characteristic of CD8<sup>+</sup> cytolytic effector differentiation.

### **Dominant bone marrow T-cell clones are present within peripheral blood TCR $\beta$ repertoires**

To investigate whether expansion was a feature of selected bone marrow T-cell clones, we determined the corresponding peripheral blood TCR $\beta$  repertoires from five patients with substantial clonal T-cell expansion in the bone marrow. We detected a total of 259837 peripheral blood T-cell clones (on average 51967 clones per patient). The most expanded peripheral blood

clone of each patient accounted for on average 8.0% of reads (range 4.0%-15.0%). 163 of 186 expanded bone marrow T-cell clones were also detectable in peripheral blood (Fig. 2A). On average, 90% of expanded bone marrow T-cell clones from each patient overlapped with peripheral blood (Fig. 2B), and clonal overlap within patient MM160 is detailed as an example (Fig. 2C). Clones with frequencies above 0.95% of total bone marrow T cells were always detectable and proportionally represented within peripheral blood TCR $\beta$  repertoires (Fig. 2D). Whether detection of dominant bone marrow T-cell clones in peripheral blood was due to hemodilution of bone marrow aspirate specimens or indicated physiological circulation within peripheral blood cannot be concluded from our data. However, high frequencies of usually bone marrow-resident multiple myeloma plasma cells (on average 29.1%, range 20.8-50.4% of total cells) within the aspirate specimens confirmed high representation of cells of the bone marrow immune microenvironment (Suppl. Fig. S5).

### **Only one out of 68 expanded bone marrow T cell clones recognize antigen presented on multiple myeloma cells**

To determine whether expansion of dominant bone marrow T cell clones was driven by antigens selectively presented on multiple myeloma cells, we tested selected TCRs for recognition of CD38-enriched multiple myeloma and CD38-depleted non-myeloma cells (Fig. 3A). Based on their frequencies, we chose a total of 68 dominant bone marrow T-cell clones from five patients with substantial clonal T-cell expansion (Fig. 3B, Suppl. Table S3). The selected clones accounted for, on average, 3.4% (range 0.6-19%) of CD8 $^{+}$  T cells. TCRs were expressed on 58 $\alpha^{-}\beta^{-}$  reporter T cells and named “58-name of the TCR”. GFP expression and IL2 production indicated T-cell activation. When stimulated with plate-bound anti-CD3 (positive control), all

TCR-recombinant cell lines produced GFP and IL2 (Suppl. Fig. S6). Upon incubation with their corresponding CD38-enriched multiple myeloma cells, three TCR-transgenic cell lines (58-14F10 and 58-15G9 from MM008, and 58-16A2 from MM160, Suppl. Table S3) produced GFP above background (58-16A2 in Fig. 3C, gating and all patients in Suppl. Fig. S7, co-culture conditions in Suppl. Table S4). Significant IL2 production was observed only from 58-16A2. Activation of 58-16A2 with CD38-depleted non-myeloma cells was due to the remaining 23.4% CD38<sup>++</sup>CD138<sup>+</sup> multiple myeloma cells, and potentially other B lineage cells, after magnetic cell separation (Suppl. Table S5), which was confirmed by repeating the enrichment (Fig. 3D) and eliminating the remaining multiple myeloma/B lineage cells from MACS CD38-depleted bone marrow by subsequent FACS (Fig. 3E, gating in Suppl. Fig. S8). The resulting population was named “FACS CD38-depleted BM,” and neither GFP nor IL2 production could be detected upon incubation with 58-16A2; only CD38-enriched multiple myeloma cells (85.6% CD38<sup>++</sup>CD138<sup>+</sup>) activated 58-16A2 (Fig. 3F). The two other TCR-recombinant cell lines that potentially recognized multiple myeloma cells (58-15G9 and 58-14F10 from MM008) showed very low GFP expression (< 1.2%) and did not produce IL2 upon incubation with CD38-enriched cells (Suppl. Fig. S7). Therefore, we could not confirm that these two T-cell clones were multiple myeloma-reactive.

In contrast to the dominant immune phenotypes of expanded bone marrow T cells outlined above (CD57<sup>+</sup>PD-1<sup>-</sup>TIM-3<sup>-</sup>), 16A2 was CD57<sup>-</sup>TIM-3<sup>+</sup> and 15G9 was PD-1<sup>+</sup> (Suppl. Fig. S9). TCR $\beta$  CDR3 sequences of all three clones (16A2 from MM160; 15G9 and 14F10 from MM008) were detectable in peripheral blood TCR $\beta$  repertoires. To determine whether non-reactivity of the majority of re-expressed dominant TCRs with bone marrow cells was due to the sensitivity of 58 $\alpha\beta$  reporter cell lines, a total of 21 TCRs from patients MM050 and MM139 were also

expressed in healthy donor peripheral blood lymphocytes. None of the TCR-transduced lymphocytes recognized antigens selectively presented on multiple myeloma cells, confirming our results obtained with 58 $\alpha\beta$  reporter cell lines (Suppl. Fig. S10).

### Multiple myeloma-reactive expanded bone marrow T-cell clones recognize self-antigens

The identification of one expanded T cell clone (16A2) that recognized CD38-enriched multiple myeloma cells and two additional clones (15G9, 14F10) with potentially similar cell type specificities raised the question of which antigens caused their expansion *in vivo*. Epitopes derived from chronically persistent viruses and neoantigens have been shown to be drivers of clonal T-cell expansion (10,37). Indeed, TCR $\alpha$  or  $\beta$  chains from 6 out of the 68 selected dominant T-cell clones had been deposited in VDJdb and reported to be specific for cytomegalovirus (CMV)- or influenza A-derived epitopes; however, paired TCR $\alpha\beta$  information was not publicly available (38). We identified the corresponding TCR chains and confirmed the specificity of three TCRs (15E10 from MM008, 10F7 from MM139, and 13G1 from MM157) for CMV epitopes (Suppl. Table S6, Suppl. Fig. S11). The epitope-specificities of the remaining three TCRs (18A12 from MM160, 12D1 and 13E11 from MM157), suggested by VDJdb (32), could not be confirmed and remain unknown.

Regarding neoantigens, we determined somatic non-synonymous mutations in multiple myeloma cells from nine selected patients that were representative of strong and weak clonal T-cell expansion. Neoantigen load and genes harboring mutations were representative of previously published data on treatment-naïve multiple myeloma (10), and potential neoantigen presentation was predicted bioinformatically (Suppl. Fig. S12, Suppl. Table S7). Multiple myeloma cells from

patients MM008 and MM160 contained 10 and 7 possibly presented somatic mutations, respectively, resulting in a total of 22 potential neoepitopes (Suppl. Table S8, and Suppl. Appendix for detailed mutation data). However, neither the multiple myeloma-reactive TCR 16A2 nor the two potentially multiple myeloma-reactive TCRs 15G9 and 14F10 recognized these neoepitopes (Suppl. Fig. S13), suggesting that they may be specific for self-antigens or epitopes from persistent pathogens.

Considering self-antigens as targets, we hypothesized that TCRs 15G9, 14F10, and 16A2 could recognize broadly available multiple myeloma cell lines. Of the five multiple myeloma cell lines, 58-16A2 was activated by U266B1 and JJN-3 (Fig. 4A). 58-15G9 and 58-14F10 were not activated by any of the tested cell lines (Suppl. Fig. S14) and excluded from further analysis. Surprisingly, no HLA-class I allele was shared between patient MM160, U266B1, and JJN-3 (Table 2). Nevertheless, blocking antibodies against HLA-class I and HLA-BC completely inhibited 58-16A2 activation by U266B1 and JJN-3 (Fig. 4B), suggesting that the target antigen might be presented on the HLA-B\*07 supertype, including HLA-B\*07:02 and B\*51:01, at least one of which was present in patient MM160, U266B1, and JJN-3.

To identify potential target epitopes of TCR 16A2, we used peptidome data of U266B1 in combination with gene expression data from MM160 and U266B1 applying the following criteria: the potential target epitope should be i) part of the HLA-class I peptidome of U266B1, ii) presented on the HLA-B\*07 supertype, and iii) expressed in MM160 and U266B1 (schematic in Fig. 4C). A total of 275 nonamer peptides met these criteria (Suppl. Table S9), were synthesized, loaded on L-363 as HLA-B\*07:02-expressing antigen-presenting cells, and tested for activation of 58-16A2. Only SPRPPLISV (SPR), which is part of Adapter Related Protein Complex 5 Subunit Mu 1 (AP5M1), was recognized by 58-16A2 (Fig. 4D). Although 58-16A2

was selectively activated by multiple myeloma/B lineage cells, *AP5M1* expression, determined by single-cell gene expression in patient MM160 and one additional patient as an example, was generally low and not restricted to plasma cell compartments (Fig. 4E, Suppl. Fig. S15).

### TCR 16A2 recognizes multiple myeloma cells from additional patients across a variety of HLA-C alleles

Having identified SPR as a potential self-antigen-derived target epitope, we investigated whether TCR 16A2 could recognize multiple myeloma cells in patients other than MM160. Multiple myeloma cells from seven out of ten additionally tested patients activated 58-16A2 (MM003, MM050, MM061, MM112, MM157, MM195, and MM204; Fig. 5A). Non-myeloma cells did not activate 58-16A2, except for patient MM003, of whom we did not have enough bone marrow to remove remaining multiple myeloma/B lineage cells from the CD38-depleted population by FACS. 58-16A2 activation did not follow the expected HLA-B\*07 supertype pattern (Table 1) but could be blocked by antibodies against HLA-class I and HLA-BC as shown for four patients as examples (Fig. 5B), leading us to question the assumed HLA-B\*07 supertype-restriction.

To systematically determine the HLA-restriction of TCR 16A2, we incubated 58-16A2 with U266B1 and JJN-3 after CRISPR-Cas9-mediated deletion of HLA-B or HLA-C. Only HLA-C, but not HLA-B, deletion abolished activation of 58-16A2 (Fig. 5C), excluding the previously assumed HLA-B-restriction of TCR 16A2. Subsequently, we transiently re-expressed all HLA-C alleles from all patients and cell lines that activated 58-16A2 in HLA-C-negative JJN-3. We included the null allele HLA-C\*04:09N because it was present in patient MM160. On average 17.3% of JJN-3 were transiently transfected with the respective HLA-C alleles (Suppl. Fig. S16), and activation of 58-16A2 required expression of at least one of the following HLA-C alleles:

02:02, 03:04, 04:01, 04:09N, 05:01, 07:02, or 08:02, indicated by significant GFP expression compared to mock-transfected HLA-C-negative JJN-3 (Fig. 5D). Accordingly, each of the eight patients whose multiple myeloma cells were recognized by 58-16A2 expressed at least one of these HLA-C alleles (Table 1). Because we identified an array of HLA-C alleles that could present antigens to 58-16A2, we asked, whether i) activation was due to allo-reactivity and ii) TCR 16A2 could recognize the previously identified target peptide, SPR, when presented on HLA-C. All HLA-C alleles that led to activation of 58-16A2 when expressed on JJN-3 were individually expressed in HLA-class I-negative HEK293T (Suppl. Fig. S17 for HLA-class I knock-out) and incubated with 58-16A2. Only HLA-C\*07:02, which was not expressed in patient MM160, presented SPR and activated 58-16A2 (Fig. 5E). Expression of HLA-C\*02:02, 03:04, or 08:02 did not result in activation of 58-16A2 with or without SPR peptide. Expression of HLA-C\*04:01, 04:09N, and 05:01 resulted in activation of 58-16A2 irrespective of SPR (Fig. 5F), suggesting allo- and/or self-peptide reactivity. Again, 58-16A2 activation in context of HLA-C\*04:01, 04:09N, and 05:01 could be blocked with antibodies against HLA-BC (Fig. 5G). In summary, 16A2 is a degenerate TCR that was activated by multiple myeloma cells of multiple patients in context of a variety of HLA-C alleles. None of the dominant TCRs that recognized multiple myeloma cells could be confirmed to be neoantigen-specific.

## DISCUSSION

Major findings of our study included i) clonal expansion occurred within cytolytic effector T-cell compartments, ii) dominant T-cell clones rarely recognized multiple myeloma cells, iii) multiple myeloma-reactive TCRs of dominant T-cell clones were not neoantigen-specific, and iv) 16A2 is

a self-reactive, degenerate TCR that recognizes antigens presented on multiple HLA-C alleles. Clonal T-cell expansion predominantly occurred within CD8<sup>+</sup> T cells, which is in line with findings on tumor-infiltrating T cells in other malignancies (21,39). We confirmed that bone marrow T cells in multiple myeloma showed exhausted and cytotoxic phenotypes (40-42). We also determined effector memory RA differentiation (CD45RA<sup>+</sup>CCR7<sup>-</sup>) of clonally expanded bone marrow T cell compartments, which has been associated with potent effector functions (43).

Data on immune checkpoint molecule expression in multiple myeloma are controversial (42,44). We showed that PD-1, TIM-3, and CTLA-4 were expressed on a minority of expanded T-cell clones, and only one out of 68 dominant clones reproducibly recognized multiple myeloma cells, providing experimental context for results of clinical trials applying immune checkpoint blockade in multiple myeloma (13-16,44,45). However, TIM-3 expression on one multiple myeloma-reactive dominant T-cell clone suggests that immune checkpoint modulation could be therapeutically relevant in carefully selected conditions. Future T cell-based immunotherapy approaches will potentially target low-abundance clones and include strategies in addition to disinhibition of pre-existing neoantigen-specific T cells.

Almost all dominant bone marrow T-cell clones were detectable in peripheral blood. Parallel aspiration of peripheral blood during bone marrow acquisition or circulation of bone marrow T cells in peripheral blood could be a possible explanation. Our study focused on expanded bone marrow T-cell clones, irrespective of overlap with peripheral blood as i) hematopoiesis takes place in the bone marrow, ii) circulation in peripheral blood does not exclude TCR specificity for antigens presented in the bone marrow, iii) neo-antigen-specific T-cell clones can be present in bone marrow and peripheral blood alike (10), and iv) frequencies of multiple myeloma cells

within the investigated bone marrow specimens indicated high representation of cells of the bone marrow microenvironment.

Besides potential specificity against multiple myeloma cells, bone marrow is a site of T- and B-cell memory (46), and major proportions of expanded bone marrow and circulating T-cell clones can be specific for persistent pathogens (47,48). Most patients in our study had been in contact with Epstein-Barr virus (EBV) and CMV, and we confirmed that three expanded bone marrow T-cell clones were CMV-specific. Considering data from other studies and concepts of immunological memory (9,46), we expected the number of virus-specific TCRs in our dataset to be considerably higher.

None of the dominant T-cell clones that recognized multiple myeloma cells could be confirmed to be neoantigen-specific. Neoantigen-specific T cells have mostly been identified in malignancies with high mutational burden (e.g. malignant melanoma) (6,9), and it is possible that higher neoantigen loads in pre-treated multiple myeloma could result in higher frequencies of neoantigen-specific T cells among dominant clones. We deliberately studied treatment-naïve patients to avoid therapy-induced effects on T-cell phenotypes and TCR repertoires. The number of somatic mutations within our treatment-naïve cohort was relatively low, representative of data from larger studies (10,49-51), and could be a reason for the absence of neoantigen-specific T cells within dominant clones. We assume multiple myeloma-reactive T cells to be part of less expanded bone marrow clones; however, their frequencies cannot be concluded from our study, which was specifically designed to define phenotypes and TCR sequences of dominant clones at the single-cell level. The presence of multiple myeloma-reactive T cells within less expanded compartments is further suggested by therapeutic effects of adoptively transferred, previously *in vitro* activated and expanded, bone marrow-infiltrating lymphocytes (52). In patients refractory

to multiple lines of therapy, neoantigen-specific T cells have been shown to become detectable in bone marrow and peripheral blood (10,53). Furthermore, immunoediting is likely to affect frequencies of neoantigen-specific T-cell clones (54). Potentially immunogenic mutations and multiple myeloma-specific T-cell clones should be studied in parallel at different stages of disease development including monoclonal gammopathy of undetermined significance, smoldering myeloma, treatment-naïve and pre-treated multiple myeloma in future studies.

One expanded T-cell clone (16A2) could be confirmed as multiple myeloma-reactive and was studied in detail. Whether the target antigen of TCR 16A2 was specifically presented on multiple myeloma cells cannot be concluded from our data. Especially in cases where we depleted the remaining multiple myeloma cells by FACS, we eliminated the entire B lineage compartment. CD19 was included as a sorting parameter because multiple myeloma cells can be CD19<sup>+</sup> even if the majority are CD19<sup>-</sup> (55,56). However, TCR 16A2 could not be activated by cells other than B lineage cells.

Using HLA knock-out and recombinant HLA expression, we excluded the initially assumed HLA-B\*07 supertype-restriction (57) of TCR 16A2 and identified the following activation characteristics: i) peptide-specific activation by SPR presented on HLA-C\*07:02; ii) activation by unknown target peptides presented on HLA-C\*02:02, 03:04, 08:02; and iii) allo-reactivity against HLA-C\*04:01 and 05:02. Activation by SPR required high peptide concentrations and presentation on HLA-C\*07:02, which was not present in patient MM160, questioning its role as a relevant target epitope *in vivo*. HLA-C\*04:09N was the only HLA-C allele in patient MM160 that led to 58-16A2 activation when expressed on HLA-C-negative JJN-3 cells. HLA-C\*04:09N is identical to HLA-C\*04:01, except for a frameshift mutation in its cytoplasmic domain, which has been assumed to lead to intracellular, but not cell surface, HLA expression (58). However,

HLA-C\*04:09N expression in HLA-C-negative JJN-3 and HLA-class I-negative HEK293T cells resulted in 58-16A2 activation, which could be blocked by HLA-BC-specific antibodies, suggesting TCR-HLA-peptide interaction at the cell surface. It is possible that HLA-C\*04:09N can become accessible for antigen presentation in situations of high cellular turnover and/or on selected cell types, including multiple myeloma plasma cells, which have extraordinarily high secretory activity. Independent of the role of HLA-C\*04:09N, recognition of multiple antigens in context of a variety of HLA-C alleles characterizes 16A2 as a profoundly degenerate TCR that, in patient MM160, has potentially been functionally inhibited by TIM-3-expression *in vivo*.

In conclusion, our study provides insights into immune phenotypes and targets of clonally expanded bone marrow T cells in treatment-naïve multiple myeloma. Dominant clones rarely recognized multiple myeloma cells and, in most cases, were not inhibited by expression of classical immune checkpoint molecules.

## ACKNOWLEDGEMENTS

We thank Kirstin Rautenberg at MDC Berlin for expert help with FACS sorting, Josefina Garmshausen for technical assistance, and Vivien Boldt for providing fluorescence in situ hybridization information. This work was supported by Deutsche Krebshilfe e.V. (70113355) (LH), Berliner Krebsgesellschaft e.V. (HAFF202013 MM) (LH), the German Cancer Consortium (DKTK) (LH), the European Union (ERC Advanced Grant 882963) (TB), a research fellowship from the German Research Foundation (DFG, PE 3127/1-1) (LP), and DFG EXC 2145 (SyNergy) ID 390857198 (KDo). LP is a scholar of the American Society of Hematology.

## AUTHOR CONTRIBUTIONS

CW and LH conceived the project. CW, MTH, XC, AM, HPR, KDo, TB, and LH designed experiments. CW, MFLC, MTH, XC, CB, KDi, and LH performed experiments. CW, CAS, MTH, ABH, LP, XC, CB, OP, PM, AM, EB, DB, AG, JS, HH, KDo, TB, and LH analyzed data. CW, TB, and LH wrote the manuscript with input from all authors. LH acquired funding, coordinated, and supervised the project.

## COMPETING INTERESTS

LB: Advisory Committees: Abbvie, Amgen, Astellas, Bristol-Myers Squibb, Celgene, Daiichi Sankyo, Gilead, Hexal, Janssen, Jazz Pharmaceuticals, Menarini, Novartis, Pfizer, Sanofi, Seattle Genetics; Research support Bayer and Jazz Pharmaceuticals. All other authors declare no competing financial interests.

## REFERENCES

1. Mitsiades CS, Mitsiades NS, Richardson PG, Munshi NC, Anderson KC. Multiple myeloma: a prototypic disease model for the characterization and therapeutic targeting of interactions between tumor cells and their local microenvironment. *J Cell Biochem* **2007**;101(4):950-68 doi 10.1002/jcb.21213.
2. Hansmann L, Blum L, Ju CH, Liedtke M, Robinson WH, Davis MM. Mass cytometry analysis shows that a novel memory phenotype B cell is expanded in multiple myeloma. *Cancer Immunol Res* **2015**;3(6):650-60 doi 10.1158/2326-6066.CIR-14-0236-T.
3. Mitsiades CS, Mitsiades N, Munshi NC, Anderson KC. Focus on multiple myeloma. *Cancer Cell* **2004**;6(5):439-44 doi 10.1016/j.ccr.2004.10.020.
4. Cavo M, Pantani L, Pezzi A, Petrucci MT, Patriarca F, Di Raimondo F, *et al.* Bortezomib-thalidomide-dexamethasone (VTD) is superior to bortezomib-cyclophosphamide-dexamethasone (VCD) as induction therapy prior to autologous stem cell transplantation in multiple myeloma. *Leukemia* **2015**;29(12):2429-31 doi 10.1038/leu.2015.274.
5. Moreau P, Attal M, Hulin C, Arnulf B, Belhadj K, Benboubker L, *et al.* Bortezomib, thalidomide, and dexamethasone with or without daratumumab before and after autologous stem-cell transplantation for newly diagnosed multiple myeloma (CASSIOPEIA): a randomised, open-label, phase 3 study. *Lancet* **2019**;394(10192):29-38 doi 10.1016/S0140-6736(19)31240-1.
6. Gros A, Parkhurst MR, Tran E, Pasetto A, Robbins PF, Ilyas S, *et al.* Prospective identification of neoantigen-specific lymphocytes in the peripheral blood of melanoma patients. *Nat Med* **2016**;22(4):433-8 doi 10.1038/nm.4051.

7. Gros A, Tran E, Parkhurst MR, Ilyas S, Pasetto A, Groh EM, *et al.* Recognition of human gastrointestinal cancer neoantigens by circulating PD-1+ lymphocytes. *J Clin Invest* **2019**;129(11):4992-5004 doi 10.1172/JCI127967.
8. Malekzadeh P, Yossef R, Cafri G, Paria BC, Lowery FJ, Jafferji M, *et al.* Antigen Experienced T Cells from Peripheral Blood Recognize p53 Neoantigens. *Clin Cancer Res* **2020**;26(6):1267-76 doi 10.1158/1078-0432.CCR-19-1874.
9. Oliveira G, Stromhaug K, Klaeger S, Kula T, Frederick DT, Le PM, *et al.* Phenotype, specificity and avidity of antitumour CD8(+) T cells in melanoma. *Nature* **2021**;596(7870):119-25 doi 10.1038/s41586-021-03704-y.
10. Perumal D, Imai N, Lagana A, Finnigan J, Melnekoff D, Leshchenko VV, *et al.* Mutation-derived Neoantigen-specific T-cell Responses in Multiple Myeloma. *Clin Cancer Res* **2020**;26(2):450-64 doi 10.1158/1078-0432.CCR-19-2309.
11. Alexandrov LB, Nik-Zainal S, Wedge DC, Aparicio SA, Behjati S, Biankin AV, *et al.* Signatures of mutational processes in human cancer. *Nature* **2013**;500(7463):415-21 doi 10.1038/nature12477.
12. Dhodapkar MV, Krasovsky J, Osman K, Geller MD. Vigorous premalignancy-specific effector T cell response in the bone marrow of patients with monoclonal gammopathy. *J Exp Med* **2003**;198(11):1753-7 doi 10.1084/jem.20031030.
13. Suen H, Brown R, Yang S, Weatherburn C, Ho PJ, Woodland N, *et al.* Multiple myeloma causes clonal T-cell immunosenescence: identification of potential novel targets for promoting tumour immunity and implications for checkpoint blockade. *Leukemia* **2016**;30(8):1716-24 doi 10.1038/leu.2016.84.

14. Lesokhin AM, Ansell SM, Armand P, Scott EC, Halwani A, Gutierrez M, *et al.* Nivolumab in Patients With Relapsed or Refractory Hematologic Malignancy: Preliminary Results of a Phase Ib Study. *J Clin Oncol* **2016**;34(23):2698-704 doi 10.1200/JCO.2015.65.9789.
15. Mateos MV, Blacklock H, Schjesvold F, Oriol A, Simpson D, George A, *et al.* Pembrolizumab plus pomalidomide and dexamethasone for patients with relapsed or refractory multiple myeloma (KEYNOTE-183): a randomised, open-label, phase 3 trial. *Lancet Haematol* **2019**;6(9):e459-e69 doi 10.1016/S2352-3026(19)30110-3.
16. Usmani SZ, Schjesvold F, Oriol A, Karlin L, Cavo M, Rifkin RM, *et al.* Pembrolizumab plus lenalidomide and dexamethasone for patients with treatment-naive multiple myeloma (KEYNOTE-185): a randomised, open-label, phase 3 trial. *Lancet Haematol* **2019**;6(9):e448-e58 doi 10.1016/S2352-3026(19)30109-7.
17. Racanelli V, Leone P, Frassanito MA, Brunetti C, Perosa F, Ferrone S, *et al.* Alterations in the antigen processing-presenting machinery of transformed plasma cells are associated with reduced recognition by CD8+ T cells and characterize the progression of MGUS to multiple myeloma. *Blood* **2010**;115(6):1185-93 doi 10.1182/blood-2009-06-228676.
18. Giannopoulos K, Kaminska W, Hus I, Dmoszynska A. The frequency of T regulatory cells modulates the survival of multiple myeloma patients: detailed characterisation of immune status in multiple myeloma. *Br J Cancer* **2012**;106(3):546-52 doi 10.1038/bjc.2011.575.

19. Han A, Glanville J, Hansmann L, Davis MM. Linking T-cell receptor sequence to functional phenotype at the single-cell level. *Nat Biotechnol* **2014**;32(7):684-92 doi 10.1038/nbt.2938.
20. Penter L, Dietze K, Bullinger L, Westermann J, Rahn HP, Hansmann L. FACS single cell index sorting is highly reliable and determines immune phenotypes of clonally expanded T cells. *Eur J Immunol* **2018**;48(7):1248-50 doi 10.1002/eji.201847507.
21. Penter L, Dietze K, Ritter J, Lammoglia Cobo MF, Garmshausen J, Aigner F, *et al.* Localization-associated immune phenotypes of clonally expanded tumor-infiltrating T cells and distribution of their target antigens in rectal cancer. *Oncoimmunology* **2019**;8(6):e1586409 doi 10.1080/2162402X.2019.1586409.
22. Ballhausen A, Ben Hamza A, Welters C, Dietze K, Bullinger L, Rahn HP, *et al.* Immune phenotypes and checkpoint molecule expression of clonally expanded lymph node-infiltrating T cells in classical Hodgkin lymphoma. *Cancer Immunol Immunother* **2022** doi 10.1007/s00262-022-03264-8.
23. Li H. Aligning sequence reads, clone sequences and assembly contigs with BWA-MEM. *arXiv e-prints* 2013. p arXiv:1303.3997.
24. Dobin A, Davis CA, Schlesinger F, Drenkow J, Zaleski C, Jha S, *et al.* STAR: ultrafast universal RNA-seq aligner. *Bioinformatics* **2013**;29(1):15-21 doi 10.1093/bioinformatics/bts635.
25. Cibulskis K, Lawrence MS, Carter SL, Sivachenko A, Jaffe D, Sougnez C, *et al.* Sensitive detection of somatic point mutations in impure and heterogeneous cancer samples. *Nat Biotechnol* **2013**;31(3):213-9 doi 10.1038/nbt.2514.

26. Andreatta M, Nielsen M. Gapped sequence alignment using artificial neural networks: application to the MHC class I system. *Bioinformatics* **2016**;32(4):511-7 doi 10.1093/bioinformatics/btv639.
27. Siewert K, Malotka J, Kawakami N, Wekerle H, Hohlfeld R, Dornmair K. Unbiased identification of target antigens of CD8+ T cells with combinatorial libraries coding for short peptides. *Nat Med* **2012**;18(5):824-8 doi 10.1038/nm.2720.
28. Engels B, Cam H, Schuler T, Indraccolo S, Gladow M, Baum C, *et al.* Retroviral vectors for high-level transgene expression in T lymphocytes. *Hum Gene Ther* **2003**;14(12):1155-68 doi 10.1089/104303403322167993.
29. Cohen CJ, Zhao Y, Zheng Z, Rosenberg SA, Morgan RA. Enhanced antitumor activity of murine-human hybrid T-cell receptor (TCR) in human lymphocytes is associated with improved pairing and TCR/CD3 stability. *Cancer Res* **2006**;66(17):8878-86 doi 10.1158/0008-5472.CAN-06-1450.
30. Lammoglia Cobo MF, Welters C, Rosenberger L, Leisegang M, Dietze K, Pircher C, *et al.* Rapid single-cell identification of Epstein-Barr virus-specific T-cell receptors for cellular therapy. *Cyotherapy* **2022**;24(8):818-26 doi 10.1016/j.jcyt.2022.03.005.
31. Quentmeier H, Pommerenke C, Dirks WG, Eberth S, Koeppel M, MacLeod RAF, *et al.* The LL-100 panel: 100 cell lines for blood cancer studies. *Sci Rep* **2019**;9(1):8218 doi 10.1038/s41598-019-44491-x.
32. Walz S, Stickel JS, Kowalewski DJ, Schuster H, Weisel K, Backert L, *et al.* The antigenic landscape of multiple myeloma: mass spectrometry (re)defines targets for T-cell-based immunotherapy. *Blood* **2015**;126(10):1203-13 doi 10.1182/blood-2015-04-640532.

33. Khodadoust MS, Olsson N, Wagar LE, Haabeth OA, Chen B, Swaminathan K, *et al.* Antigen presentation profiling reveals recognition of lymphoma immunoglobulin neoantigens. *Nature* **2017**;543(7647):723-7 doi 10.1038/nature21433.
34. Rappaport J, Mann M, Ishihama Y. Protocol for micro-purification, enrichment, pre-fractionation and storage of peptides for proteomics using StageTips. *Nat Protoc* **2007**;2(8):1896-906 doi 10.1038/nprot.2007.261.
35. Cox J, Mann M. MaxQuant enables high peptide identification rates, individualized p.p.b.-range mass accuracies and proteome-wide protein quantification. *Nat Biotechnol* **2008**;26(12):1367-72 doi 10.1038/nbt.1511.
36. R Core Team. R: A Language and Environment for Statistical Computing. Vienna, Austria: R Foundation for Statistical Computing; 2020.
37. Messaoudi I, Lemaoult J, Guevara-Patino JA, Metzner BM, Nikolich-Zugich J. Age-related CD8 T cell clonal expansions constrict CD8 T cell repertoire and have the potential to impair immune defense. *J Exp Med* **2004**;200(10):1347-58 doi 10.1084/jem.20040437.
38. Bagaev DV, Vroomans RMA, Samir J, Stervbo U, Rius C, Dolton G, *et al.* VDJdb in 2019: database extension, new analysis infrastructure and a T-cell receptor motif compendium. *Nucleic Acids Res* **2020**;48(D1):D1057-D62 doi 10.1093/nar/gkz874.
39. Lucca LE, Axisa PP, Lu B, Harnett B, Jessel S, Zhang L, *et al.* Circulating clonally expanded T cells reflect functions of tumor-infiltrating T cells. *J Exp Med* **2021**;218(4) doi 10.1084/jem.20200921.

40. Paiva B, Azpilikueta A, Puig N, Ocio EM, Sharma R, Oyajobi BO, *et al.* PD-L1/PD-1 presence in the tumor microenvironment and activity of PD-1 blockade in multiple myeloma. *Leukemia* **2015**;29(10):2110-3 doi 10.1038/leu.2015.79.
41. Raitakari M, Brown RD, Sze D, Yuen E, Barrow L, Nelson M, *et al.* T-cell expansions in patients with multiple myeloma have a phenotype of cytotoxic T cells. *Br J Haematol* **2000**;110(1):203-9 doi 10.1046/j.1365-2141.2000.02131.x.
42. Zelle-Rieser C, Thangavadiel S, Biedermann R, Brunner A, Stoitzner P, Willenbacher E, *et al.* T cells in multiple myeloma display features of exhaustion and senescence at the tumor site. *J Hematol Oncol* **2016**;9(1):116 doi 10.1186/s13045-016-0345-3.
43. Willinger T, Freeman T, Hasegawa H, McMichael AJ, Callan MF. Molecular signatures distinguish human central memory from effector memory CD8 T cell subsets. *J Immunol* **2005**;175(9):5895-903 doi 10.4049/jimmunol.175.9.5895.
44. Suen H, Brown R, Yang S, Ho PJ, Gibson J, Joshua D. The failure of immune checkpoint blockade in multiple myeloma with PD-1 inhibitors in a phase 1 study. *Leukemia* **2015**;29(7):1621-2 doi 10.1038/leu.2015.104.
45. Oliva S, Troia R, D'Agostino M, Boccadoro M, Gay F. Promises and Pitfalls in the Use of PD-1/PD-L1 Inhibitors in Multiple Myeloma. *Front Immunol* **2018**;9:2749 doi 10.3389/fimmu.2018.02749.
46. Chang HD, Radbruch A. Maintenance of quiescent immune memory in the bone marrow. *Eur J Immunol* **2021**;51(7):1592-601 doi 10.1002/eji.202049012.
47. Hislop AD, Annels NE, Gudgeon NH, Leese AM, Rickinson AB. Epitope-specific evolution of human CD8(+) T cell responses from primary to persistent phases of Epstein-Barr virus infection. *J Exp Med* **2002**;195(7):893-905.

48. Hislop AD, Taylor GS, Sauce D, Rickinson AB. Cellular responses to viral infection in humans: lessons from Epstein-Barr virus. *Annu Rev Immunol* **2007**;25:587-617 doi 10.1146/annurev.immunol.25.022106.141553.
49. Kortum KM, Langer C, Monge J, Bruins L, Zhu YX, Shi CX, *et al.* Longitudinal analysis of 25 sequential sample-pairs using a custom multiple myeloma mutation sequencing panel (M(3)P). *Ann Hematol* **2015**;94(7):1205-11 doi 10.1007/s00277-015-2344-9.
50. Leich E, Weissbach S, Klein HU, Grieb T, Pischimarov J, Stuhmer T, *et al.* Multiple myeloma is affected by multiple and heterogeneous somatic mutations in adhesion- and receptor tyrosine kinase signaling molecules. *Blood Cancer J* **2013**;3:e102 doi 10.1038/bcj.2012.47.
51. Walker BA, Mavrommatis K, Wardell CP, Ashby TC, Bauer M, Davies FE, *et al.* Identification of novel mutational drivers reveals oncogene dependencies in multiple myeloma. *Blood* **2018**;132(6):587-97 doi 10.1182/blood-2018-03-840132.
52. Noonan KA, Huff CA, Davis J, Lemass MV, Fiorino S, Bitzan J, *et al.* Adoptive transfer of activated marrow-infiltrating lymphocytes induces measurable antitumor immunity in the bone marrow in multiple myeloma. *Sci Transl Med* **2015**;7(288):288ra78 doi 10.1126/scitranslmed.aaa7014.
53. Noonan K, Matsui W, Serafini P, Carbley R, Tan G, Khalili J, *et al.* Activated marrow-infiltrating lymphocytes effectively target plasma cells and their clonogenic precursors. *Cancer Res* **2005**;65(5):2026-34 doi 10.1158/0008-5472.CAN-04-3337.
54. Nakamura K, Smyth MJ, Martinet L. Cancer immunoediting and immune dysregulation in multiple myeloma. *Blood* **2020**;136(24):2731-40 doi 10.1182/blood.2020006540.

55. Hansmann L, Han A, Penter L, Liedtke M, Davis MM. Clonal Expansion and Interrelatedness of Distinct B-Lineage Compartments in Multiple Myeloma Bone Marrow. *Cancer Immunol Res* **2017**;5(9):744-54 doi 10.1158/2326-6066.CIR-17-0012.
56. Nerreter T, Letschert S, Gotz R, Doose S, Danhof S, Einsele H, *et al.* Super-resolution microscopy reveals ultra-low CD19 expression on myeloma cells that triggers elimination by CD19 CAR-T. *Nat Commun* **2019**;10(1):3137 doi 10.1038/s41467-019-10948-w.
57. Sidney J, Peters B, Frahm N, Brander C, Sette A. HLA class I supertypes: a revised and updated classification. *BMC Immunol* **2008**;9:1 doi 10.1186/1471-2172-9-1.
58. Balas A, Santos S, Aviles MJ, Garcia-Sanchez F, Lillo R, Alvarez A, *et al.* Elongation of the cytoplasmic domain, due to a point deletion at exon 7, results in an HLA-C null allele, Cw\*0409 N. *Tissue Antigens* **2002**;59(2):95-100 doi 10.1034/j.1399-0039.2002.590204.x.

**TABLES****Table 1**

Patient	Age (years)	Sex	BM infiltration (%)	ISS stage	Disease type	CMV IgG	EBV VCA- IgG	HLA-class I
MM195	47	female	60-70	II	IgG κ	neg	pos	A*01:01; A*02:01 B*27:05; B*44:02 C*02:02; C*05:01 A*03:01; A*24:02
MM104	69	female	30-40	III	λ light chain	pos	pos	B*51:01; B*55:01 C*01:02; C*03:03
MM078	41	male	60	II	IgG κ	pos	pos	A*02:01; A*23:01 B*15:03; B*15:03
MM165	66	female	90	III	κ light chain	neg	pos	C*02:10; C*02:10 A*01:01; A*02:01 B*51:01; B*08:01 C*02:02; C*07:01
MM061	64	male	30	III	λ light chain	neg	neg	A*26:01; A*32:01 B*44:02; B*38:01 C*05:01; C*12:03
MM112	40	female	95	III	IgA λ	neg	pos	A*03:01; A*24:02 B*07:02; B*51:01 C*01:02; C*07:02
MM204	61	female	70	III	λ light chain	neg	pos	A*02:01; A*29:02 B*08:01; B*44:02 C*05:01; C*07:18
MM008	86	male	70	II	IgG κ	n.d.	n.d.	A*01:01; A*03:01 B*07:02; B*08:01 C*07:01; C*07:02
MM003	71	male	60	II	IgG κ	pos	n.d.	A*01:01; A*30:02 B*08:01; B*35:03 C*04:01; C*07:01
MM157	83	male	80	II	IgG κ	neg	pos	A*03:01; A*11:01 B*07:02; B*44:02 C*05:01; C*07:02
MM050	85	female	50	III	IgG λ	pos	pos	A*03:01; A*03:01 B*07:02; B*51:01 C*01:02; C*07:02
MM139	73	female	70	II	IgG κ	pos	pos	A*01:01; A*24:02 B*15:17; B*35:01 C*04:29; C*07:01
MM160	68	female	25	III	IgA κ	pos	pos	A*02:01; A*23:01 B*44:03; B*51:01 C*15:02; C*04:09N

**Table 1. Patient characteristics**

Bone marrow plasma cell infiltration was determined by histology. BM, bone marrow; ISS, international staging system; CMV, cytomegalovirus; EBV, Epstein-Barr virus; VCA, virus capsid antigen; and n.d., not determined. Genetic characteristics can be found in Supplementary Table S1.

**Table 2**

<i>HLA-class I</i>	<i>MM160</i>	<i>U266B1</i>	<i>JJN-3</i>	<i>L-363</i>	<i>NCI-H929</i>	<i>KMS-12-PE</i>
A	02:01; 23:01	02:01; 03:01	03:01; 33:01	02:01; 31:01	03:01; 24:02	26:01; 33:03
B	44:03; 51:01	07:02; 40:01	07:02; 14:02	07:02; 40:01	07:02; 18:01	35:01; 44:03
C	15:02; 04:09N	03:04; 07:02	07:02; 08:02	03:04; 07:02	07:02; 07:02	03:03; 14:03

**Table 2. HLA types of patient MM160 and multiple myeloma cell lines**

HLA type of MM160 was determined by sequencing. All cell line HLA types were downloaded from TRON Cell Line Portal (<http://www.celllines.tron-mainz.de>).

**FIGURE LEGENDS****Figure 1. Clonal expansion-associated phenotypes of bone marrow T cells.**

(A) Parallel determination of TCR $\alpha\beta$  sequences, transcription factors, and cytokine gene expression from amplified cDNA of single FACS-sorted T cells. Single cells are arranged in columns with each column representing one cell. The top bar indicates TCR sequences; adjacent cells with the same color in the top bar indicate identical TCR $\alpha\beta$  CDR3 amino acid sequences. Clonal expansion was defined as the detection of at least two cells with identical TCR $\alpha\beta$  CDR3 sequences. The upper part of the heatmap indicates single cell gene expression determined by targeted panel sequencing. The lower part of the heatmap visualizes corresponding FACS index sort data. The heatmaps show data from patients MM160 and MM061 as examples for strong and weak clonal T-cell expansion, respectively. (B) Absolute numbers of expanded bone marrow T-cell clones per patient ( $n=13$ ). Patients were ordered by size of the most expanded clone per patient as shown in panel D. (C) Percentages of expanded T-cell clones expressing CD8 or CD4. Data points indicate individual patients. (D) Frequencies of expanded CD8 $^{+}$  T-cell clones within CD8 $^{+}$  T cells. Each data point represents one unique T-cell clone. (E) Immune phenotypes of CD8 $^{+}$  expanded and non-expanded T-cell clones determined by FACS index sorting. Data from all 13 patients are summarized as box plots, and data points indicate individual patients. BTLA and CD28 were stained in  $n=12$ ; CD38, CTLA-4, and TIM-3 in  $n=11$ ; and CD39 in  $n=3$  (out of 13 patients). A clone was determined positive for the indicated parameter if the majority of cells belonging to this clone were positive. (F) Gating example for patient MM160. Each data point represents one T-cell belonging to an expanded (black) or non-expanded (red) clone. Numbers within gates indicate percentages. (G) Single-cell gene expression of selected cytokines and transcription factors that were detected in more than 5% of expanded or non-expanded CD8 $^{+}$  T

cells. Data points represent individual patients. All panels show data from n=13 patients, unless otherwise stated. Single-cell FACS and sequencing for each patient were done once resulting in n=13 experiments. Box plots represent 25<sup>th</sup> to 75<sup>th</sup> percentiles, lines within boxes indicate medians. Statistical significance was calculated using two-sided Wilcoxon test, \*p<0.05, \*\*p<0.005, \*\*\*p<0.0005

## Figure 2. Circulation of expanded bone marrow T-cell clones in peripheral blood.

(A) Overlap of matched expanded bone marrow and total peripheral blood T-cell clones from 5 patients. Numbers indicate total numbers of T-cell clones. (B) Total numbers of expanded bone marrow clones that were also detectable in peripheral blood for each individual patient. (C) Left: single-cell TCR $\alpha\beta$  sequencing data of bone marrow T cells from patient MM160. Cells that belonged to the same T cell clone were arranged next to each other and represented by identical colors. Clones are ordered by size, and non-expanded T cells with unique TCR $\alpha\beta$  sequences are represented in grey. Right: corresponding peripheral blood TCR $\beta$  repertoire sequencing data. T-cell clones are ordered by TCR $\beta$  read number. Clones with a frequency below 0.3% are represented in grey. Links connect bone marrow T-cell clones to peripheral blood T-cell clones with identical CDR3 $\beta$  amino acid sequences (black links: expanded bone marrow T-cell clones, grey links: non-expanded bone marrow T-cell clones). (D) Spearman correlation of clonal T-cell expansion in bone marrow and peripheral blood for all 5 sample pairs combined. Bone marrow T-cell clones with a frequency above 0.95% (vertical black line) were always detectable in corresponding peripheral blood. The grey area indicates 95% confidence interval for an assumed linear correlation (blue line). Sequencing of bone marrow and peripheral blood T cells was done

once for each patient resulting in n=5 experiments. BM, bone marrow; PB, peripheral blood; and ND, not detected.

### Figure 3. Recognition of multiple myeloma cells by dominant bone marrow T cell clones

(A) Experimental setup: From five patients with substantial bone marrow T cell expansion, 68 clones were selected for TCR expression in 58 $\alpha^- \beta^-$  reporter T cells and healthy donor peripheral blood lymphocytes. TCR-recombinant cells were incubated with respective CD38-enriched multiple myeloma or CD38-depleted non-myeloma cells for 16 hours at 37 °C 5% CO<sub>2</sub> to determine antigen recognition. (B) Patients and T-cell clones that were selected for expression (red) based on their frequencies. Data points indicate T-cell clones. Clones of mentioned in the manuscript are labeled. (C) Incubation of TCR-recombinant 58 $\alpha^- \beta^-$  reporter T cells with enriched multiple myeloma and non-myeloma cells from patient MM160. 58 $\alpha^- \beta^-$  cells expressing an HLA-A\*02:01-restricted TCR specific for the EBV-derived peptide GLCTLVAML (GLC) were incubated for 16 hours at 37 °C 5% CO<sub>2</sub> with myeloma and non-myeloma cells from the same patient loaded with the target peptide as control (ctrl). GFP and murine IL2 were measured as readouts for T-cell activation. (D) MACS CD38-enrichment and depletion of bone marrow from patient MM160. Cells were pre-gated on mononuclear cells. To remove remaining multiple myeloma cells (CD38<sup>++</sup>CD38<sup>+</sup>) from MACS CD38-depleted cells, (E) we performed subsequent FACS (CD19 $^-$ CD38 $^-$ CD138 $^-$ , sorting gates in Suppl. Fig. S8), resulting in 0.0% remaining CD38<sup>++</sup>CD138<sup>+</sup> multiple myeloma cells within the FACS CD38-depleted BM population. (F) Repeated incubation of 58-16A2 with CD38-enriched and FACS CD38-depleted bone marrow from patient MM160 or 58-16A2 alone. Cells were pre-gated on single live murine CD3 $^+$  T cells after exclusion of human bone marrow cells by scatter characteristics, CD38, CD138, and CD45

staining. For each patient, incubations of reporter cells with CD38-enriched or depleted bone marrow cells were done in one experiment resulting in n=5 experiments, unless stated otherwise. BM, bone marrow; PBL, peripheral blood lymphocytes; and n.d., not detectable.

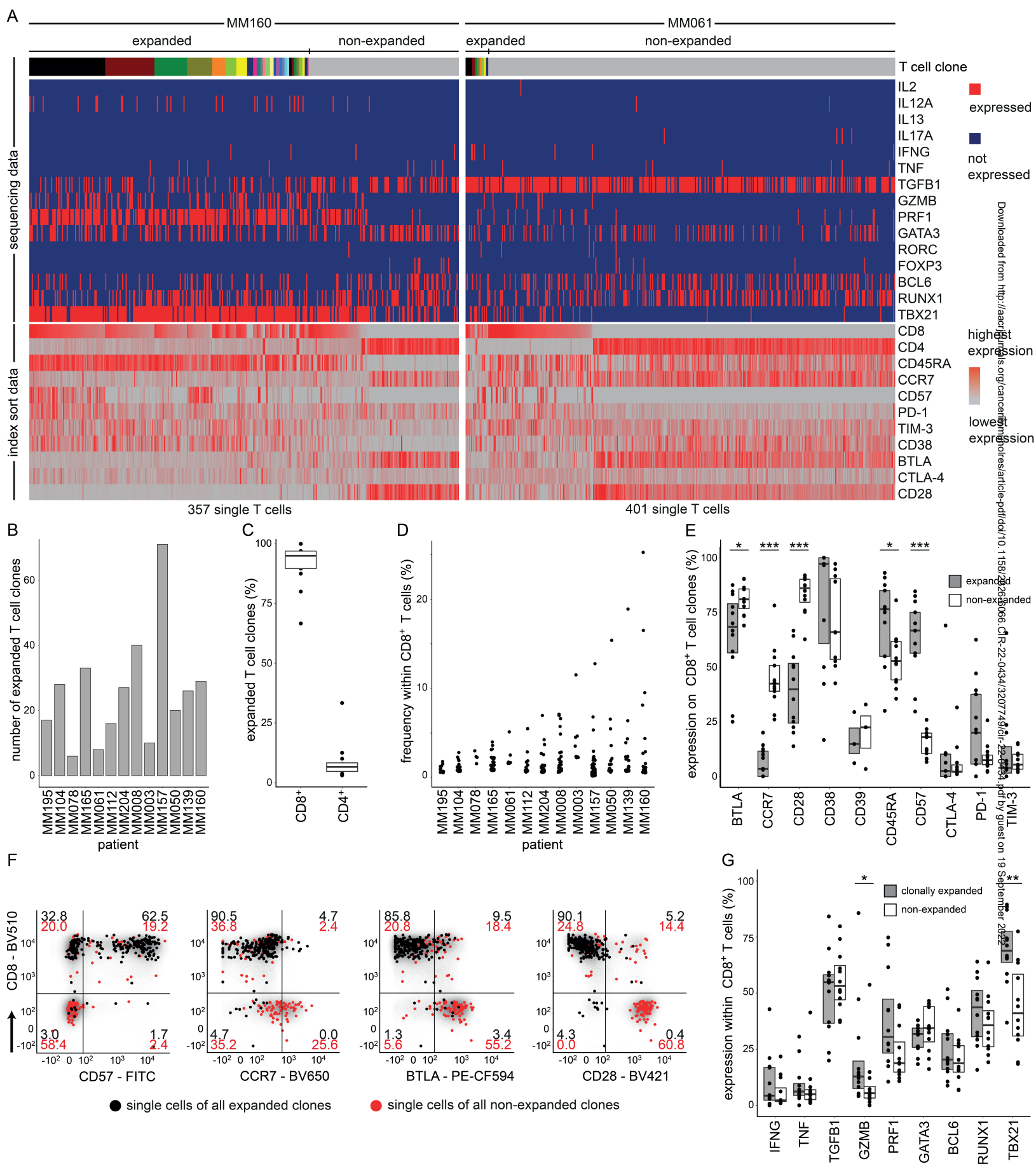
**Figure 4. TCR 16A2 recognizes the AP5M1-derived peptide SPRPPLISV (SPR).**

(A, B)  $3 \times 10^4$  58-16A2 were incubated with  $5 \times 10^4$  cells of different multiple myeloma cell lines for 16 hours at 37 °C 5% CO<sub>2</sub>. Blocking antibodies against HLA-class I, HLA-A\*02, or HLA-BC were used at 20 µg/mL, 20 µg/mL, or 40 µg/mL, respectively. (C) Potential target peptides of 16A2 were selected from a total of 3686 nonamer peptides of the U266B1 peptidome applying the following criteria: i) RNA expression within multiple myeloma cells of MM160 and U266B1, and ii) presentation on HLA-B\*07:02 and HLA-B\*51:01. Peptides with predicted HLA binding affinity  $\leq$  700 nM (NetMHC) were considered presented. (D) L-363 cells that did not activate 58-16A2 without additional peptide loading were used as antigen-presenting cells. RPR (amino acid sequence: RPRPPVLSV) was used as a negative control peptide representative for all other 274 nonamer peptides that did not activate 58-16A2. (E) Combined single-cell gene expression of CD38-enriched multiple myeloma bone marrow and peripheral blood cells from patient MM160. Each data point represents one out of 4430 single cells. Left: Multiple myeloma cells were identified by monoclonal immunoglobulin light chain CDR3 sequences. Right: *AP5M1* expression was generally low and not restricted to multiple myeloma cells. A, B, and D indicate mean  $\pm$  standard deviation. Data are representative of n=3 experiments unless otherwise stated.

**Figure 5. 16A2 is a degenerate TCR that recognizes multiple myeloma cells of different patients in context of a variety of HLA-C alleles.**

(A) 58-16A2 were incubated with CD38-enriched multiple myeloma or MACS CD38-depleted non-myeloma cells. Axis descriptions of patients who activated 58-16A2 are highlighted by red rectangles. “Non-myeloma BM cells” represent CD38-depleted bone marrow (BM). In patients MM157 and MM195, remaining multiple myeloma/B lineage cells were removed from MACS CD38-depleted bone marrow by additional FACS sorting (sorting criteria: CD38<sup>-</sup>CD138<sup>-</sup>CD19<sup>-</sup>, gating in Suppl. Fig. S8). (B) 58-16A2 were incubated for 16 hours at 37 °C 5% CO<sub>2</sub> with multiple myeloma cells from four patients in presence of blocking antibodies against HLA-class I or HLA-BC. (C) 58-16A2 were incubated with JJN-3 or U266B1 cells for 16 hours at 37 °C 5% CO<sub>2</sub>. HLA-B or HLA-C were deleted using CRISPR-Cas9. (D) 58-16A2 were incubated for 16 hours at 37 °C 5% CO<sub>2</sub> with HLA-C-negative JJN-3 transiently transfected with selected HLA-C alleles. Wild-type, un-manipulated JJN-3 expressing all endogenous HLA alleles; Mock, nucleofection of HLA-C-negative JJN-3 without HLA-containing plasmid. Statistical significance between mock and indicated conditions was determined by paired Student’s t-test. \*p<0.05, \*\*p<0.01, \*\*\*p<0.001. (E-G) Selected HLA-C alleles were expressed in HLA-class I-negative HEK293T cells and incubated with 58-16A2 for 16 hours at 37 °C 5% CO<sub>2</sub>. Mock, transfection without HLA-containing plasmid. (E) HLA-recombinant HEK293T were also loaded with SPR. (G) Blocking antibodies against HLA-BC or an isotype antibody were added before co-incubation. Bar charts indicate mean ± standard deviation. Data are representative of n=3 experiments.

Figure 1



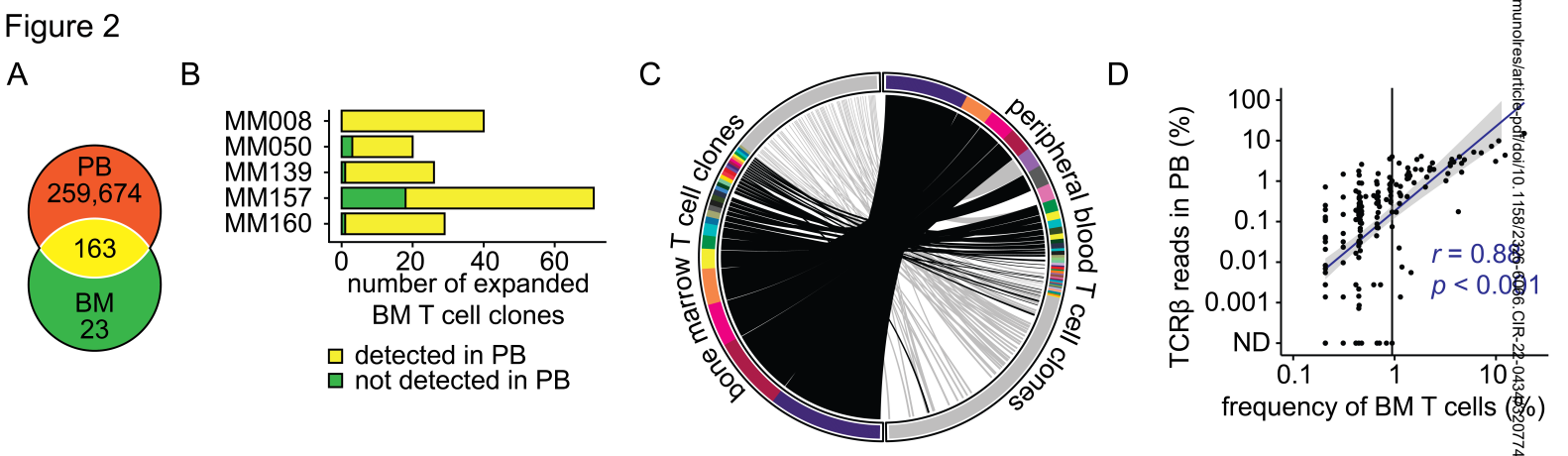
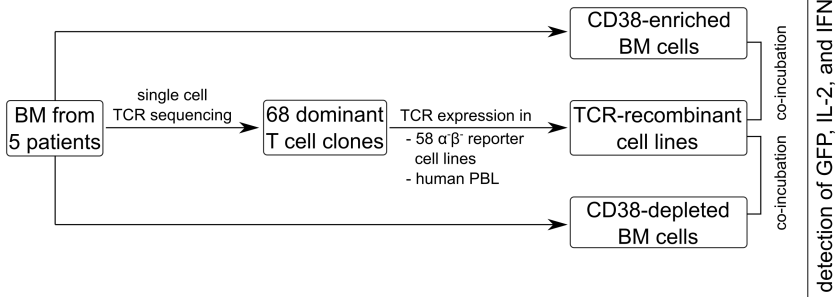
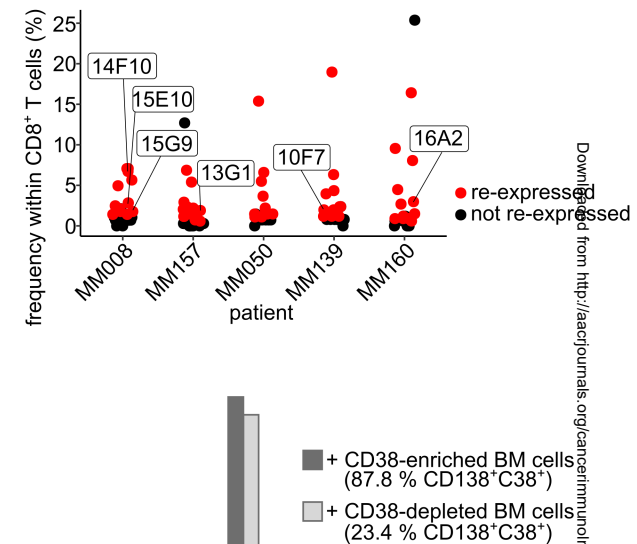


Figure 3

A

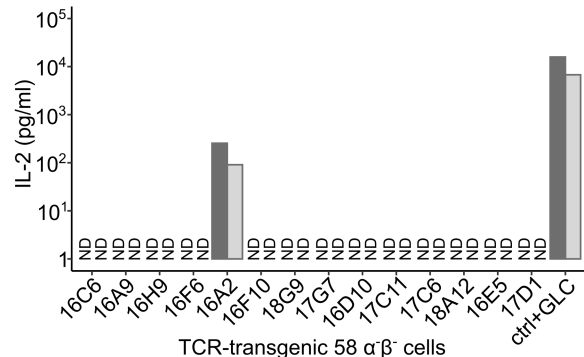
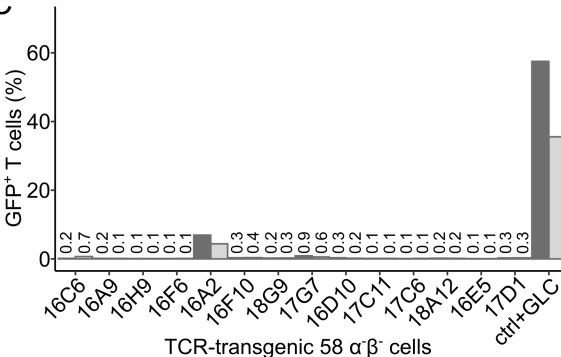


B

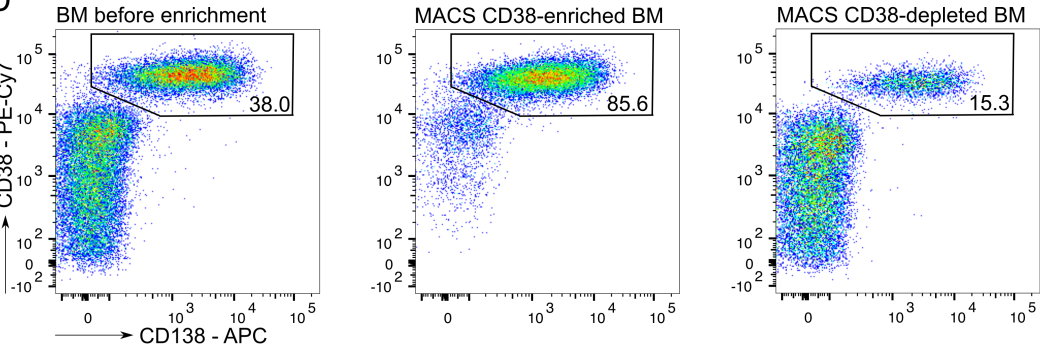


Downloaded from <http://aacjournals.org/cancerimmunores/article-pdf/doi/10.1158/2326-6066.CIR-22-0434/3207749/cir-22-0434.pdf> by guest on 19 September 2023

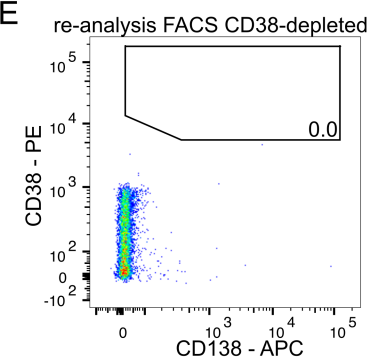
C



D



E



F

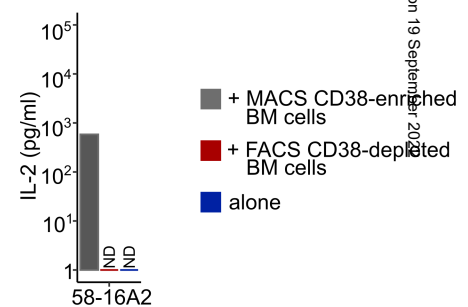
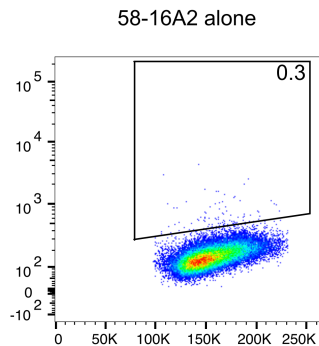
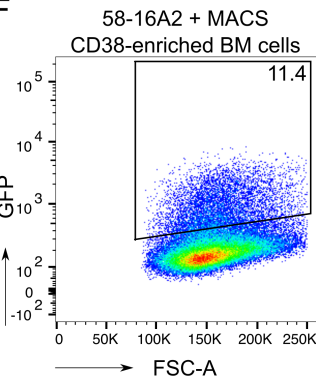
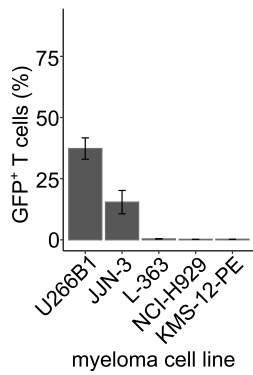
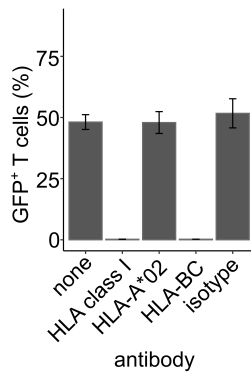


Figure 4

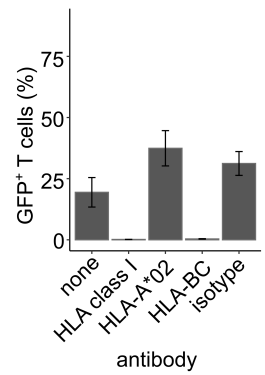
A 58-16A2 + myeloma cell lines



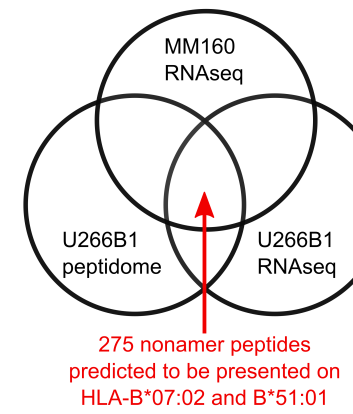
B 58-16A2 + U266B1



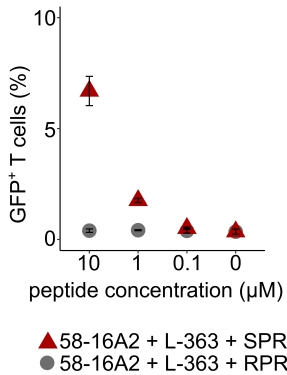
58-16A2 + JJN-3



C



D



E

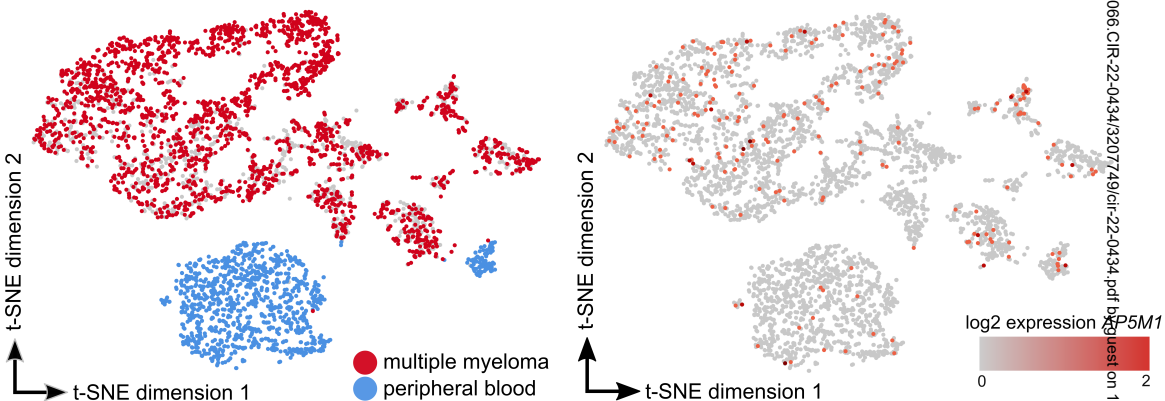


**Figure 5**